Efficient heterologous expression, functional characterization and molecular modeling of annular seabream digestive phospholipase A2

Nabil Smichi, Houcemeddine Othman, Neila Achouri, Alexandre Noiriel, Soumaya Triki, Vincent Arondel, Najet Srairi-Abid, Abdelkarim Abousalham, Youssef Gargouri, Nabil Miled, et al.

Title: Efficient heterologous expression, functional characterization and molecular modeling of annular seabream digestive phospholipase A_2

Authors: Nabil Smichi, Houcemeddine Othman, Neila Achouri, Alexandre Noiriel, Soumaya Triki, Vincent Arondel, Najet Srairi-abid, Abdelkarim Abousalham, Youssef Gargouri, Nabil Miled, Ahmed Fendri

PII: S0009-3084(16)30206-7
DOI: http://dx.doi.org/doi:10.1016/j.chemphyslip.2017.06.004
Reference: CPL 4568

To appear in: *Chemistry and Physics of Lipids*

Received date: 16-12-2016
Revised date: 19-4-2017
Accepted date: 13-6-2017

Please cite this article as: Smichi, Nabil, Othman, Houcemeddine, Achouri, Neila, Noiriel, Alexandre, Triki, Soumaya, Arondel, Vincent, Srairi-abid, Najet, Abousalham, Abdelkarim, Gargouri, Youssef, Miled, Nabil, Fendri, Ahmed, Efficient heterologous expression, functional characterization and molecular modeling of annular seabream digestive phospholipase A2.Chemistry and Physics of Lipids http://dx.doi.org/10.1016/j.chemphyslip.2017.06.004

Efficient heterologous expression, functional characterization and molecular modeling of annular seabream digestive phospholipase A_2

Nabil Smichi[a,b], Houcemeddine Othman[c], Neila Achouri[a], Alexandre Noiriel[d], Soumaya Triki[e], Vincent Arondel[f], Najet Srairi-abid[c], Abdelkarim Abousalham[d], Youssef Gargouri[a], Nabil Miled[a] and Ahmed Fendri[a*]

[a] University of Sfax, Laboratory of Biochemistry and Enzymatic Engineering of Lipases, ENIS, BP 3038 Sfax-Tunisia. Tel/Fax: + 216 74675055.

[b] CNRS, Enzymologie Interfaciale et Physiologie de la Lipolyse, Aix-Marseille University, UMR7282, 31 chemin Joseph Aiguier, 13402 Marseille Cedex 20, France

[c] University Tunis-ElManar, Institute of Pasteur, Laboratory of Venoms and Therapeutiques Biomolecules LR11IPT08, Tunis 1002, Tunisia;

[d] Univ Lyon, Université Lyon 1, Institut de Chimie et de Biochimie Moléculaires et Supramoléculaires, UMR 5246, Métabolisme, Enzymes et Mécanismes Moléculaires (MEM2), 43, Bd du 11 novembre 1918, F-69622 Villeurbanne cedex, France;

[e] University of Sfax, Laboratory of Molecular and Cellular Screening Processes, Center of Biotechnology of Sfax, BP 1117, Route Sidi Mansour Km 6, Sfax, Tunisia.;
[f] Laboratoire de biogenèse Membranaire, CNRS, UMR5200, INRA Bordeaux Aquitaine, BP81, 71 Edouard Bourlaux, 33883 Villenave d'Ornon cedex, Bordeaux, France.

* **Correspondence address:** Dr. Ahmed Fendri, Laboratory of Biochemistry and Enzymatic Engineering of Lipases, ENIS, Sfax-Tunisia. Tel/Fax: + 216 74675055.

Email: ahmed_fendri @yahoo.fr

Graphical abstract

3D structure of sparidae PLA_2s

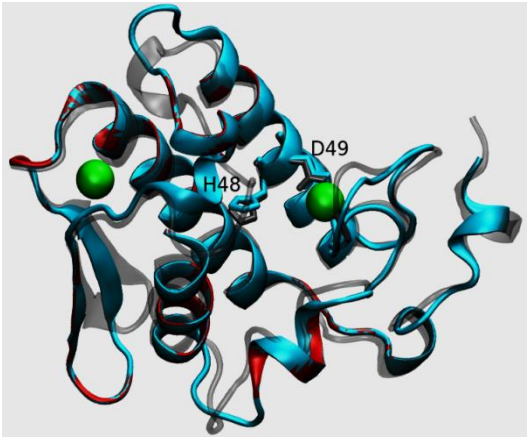

$AsPLA_2$ activity toward phospholipids

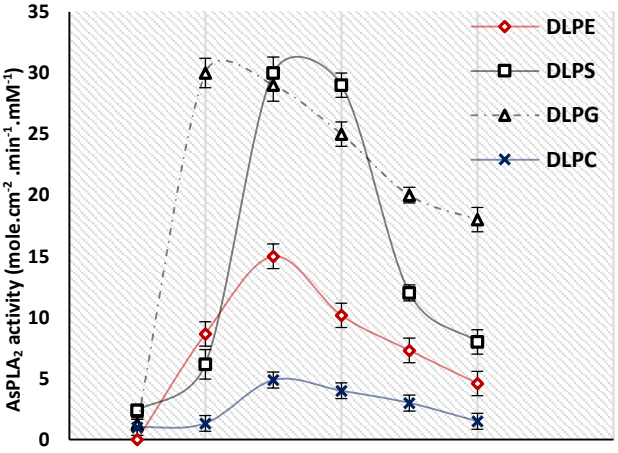

Highlights

- • Five fish digestive $sPLA_2$s cDNAs were synthesized by RT-PCR.
- • Phylogenetic studies of fish $sPLA_2$s show a close homology to bird pancreatic $sPLA_2$s.
- The expressed $AsPLA_2$ was highly purified and was found to be thermoactive.
- • 3-D structure models of annular and white seabream $sPLA_2$s were built.
- • The higher thermoactivity and phospholipids specificity of $AsPLA_2$ was explained.

Abstract

Here we report the cDNA cloning of a phospholipase A_2 (PLA_2) from five Sparidae species. The deduced amino acid sequences show high similarity with pancreatic PLA_2. In addition, a phylogenetic tree derived from alignment of various available sequences revealed that Sparidae PLA_2 are closer to avian PLA_2 group IB than to mammals' ones. In order to understand the structure-function relationships of these enzymes, we report here the recombinant expression in *E.coli*, the refolding and characterization of His-tagged annular seabream PLA_2 ($AsPLA_2$). A single Ni-affinity chromatography step was used to obtain a highly purified recombinant $AsPLA_2$ with a molecular mass of 15 kDa as attested by gel electrophoresis and MALDI-TOF mass spectrometry data. The enzyme has a specific activity of 400 $U.mg^{-1}$ measured on phosphatidylcholine at pH 8.5 and 50°C. The enzyme high thermo-activity and thermo-stability make it a potential candidate in various biological applications. The 3D structure models of these enzymes were compared with structures of phylogenetically related pancreatic PLA_2. By following these models and utilizing molecular dynamics simulations, the resistance of the $AsPLA_2$ at high temperatures was explained. Using the monomolecular film technique, $AsPLA_2$ was found to be active on various phospholipids spread at the air/water interface at a surface pressure between 12 and 25 $dynes.cm^{-1}$. Interestingly, this enzyme was shown to be mostly active on dilauroyl-phosphatidylglycerol monolayers and this behavior was confirmed by molecular docking and dynamics simulations

analysis. The discovery of a thermo-active new member of Sparidae PLA_2, provides new insights on structure-activity relationships of fish PLA_2.

Keywords: Sparidae; ; ; ; ; , phospholipase A_2 cloning, phylogeny, expression and purification, monomolecular film technique, structural characterization.

1. Introduction

Secreted phospholipases A_2 ($sPLA_2$) (EC 3.1.1.4) are a family of ubiquitous soluble enzymes which can be found in a variety of tissues, not only in pancreatic juice, where, incidentally, only a single member of $sPLA_2$ family is highly abundant [1,2]. This family has a distinctive high capacity to catalyze the hydrolysis of the ester bond of the fatty acids esterified at the *sn*-2 position of membrane glycerophospholipids generating free fatty acid and lysophospholipids [1]. $sPLA_2$ isoforms generally have a molecular mass ranging from 14 to 19 kDa, except the one for Group III that have a molecular mass of 55 kDa [3,4]. $sPLA_2$ are subdivided into ten groups based on theirs structures, catalytic mechanisms, localizations and grouped according to their pattern of disulfide bonds [4]. They usually contain 6-8 disulfide bonds [1,4]. Pancreatic $sPLA_2$ is in the group IB ($sPLA_2$-GIB) and plays a central role in the digestion of dietary phospholipids [4]. It is stored in the form of an inactive pro-$sPLA_2$ (zymogen) in the secretory granules of pancreatic acinar cells. Pro-$sPLA_2$ is activated through limited tryptic proteolysis in the intestinal tract into its active form [3].

$sPLA_2$s from mammals share common molecular structural features such as two conserved central α-helices containing the catalytic pair His/Asp and a hydrogen-bonding network connecting the interfacial binding site, the catalytic and the calcium binding sites [3-5]. The pancreatic $sPLA_2$s have an N-terminal prepropeptide in their sequence and are consequently secreted from cells [1,4]. The $sPLA_2$-GIB possesses additional features such as the presence of the so-called pancreatic loop, whereas they are devoided from C-terminal extension such some other $sPLA_2$.

Calcium is absolutely required for hydrolysis and it binds with the conserved carbonyl oxygens of the tyrosine and glycine from the calcium binding loop. The primary structures of mammalian group IB $sPLA_2$s have been determined, and their physicochemical properties and reaction mechanisms have been extensively studied [6,7].

In contrast to mammalian $sPLA_2$, there is a paucity of information about the enzymology and the structure of fish PLA_2 [7, 8]. Infante and Cahu [8] have determined the primary structure of a $sPLA_2$, belonging to the group IB, from the digestive tract of the seabass (*Dicentrarchus labrax*). The mRNA expression levels and enzymatic activity of this $sPLA_2$ were stimulated by increased phospholipid contents in the diet [8,9]. Recently, Sæle *et al.* [10] sequenced and described the primary structure of a group IB $sPLA_2$ from Atlantic cod (*Gadus morhua*).

The Sparidae, named also seabreams, are among the most valuable fishes, not only for small-scale and semi-industrial fisheries but also for aquaculture throughout the Mediterranean Sea [11]. They are represented in Mediterranean Sea by 22 species that usually inhabit coastal areas, and produce pelagic larvae [11]. In common with many other fishes, Sparidae seabreams share a major tissue, pyloric caeca, containing digestive enzymes [12,13]. This digestive tissue constitutes an adaptation to increase gut surface area and the site of lipid absorption [12, 13]. In previous works, many fish species from the Sparidae family have been investigated with regards to reproduction and growth. However, little information is available concerning structure-function relationships for Sparidae digestive PLA_2.

In this work, we cloned cDNA encoding mature PLA_2 from five Sparidae species. Phylogenetic trees were built based on these sequences and those of $sPLA_2$s from other vertebrates. We report also the expression of the His-tagged annular seabream PLA_2 ($AsPLA_2$) in *Escherichia coli*. The recombinant enzyme was purified and its enzymatic activity was characterized on phosphatidylcholine (PC) substrates in the form of emulsion or monomolecular film using the monolayer technique. Structural models of Sparidae PLA_2s were built and allowed us to study of structure–function relationships of these fish enzymes.

2. Materials and Methods

2.1. Sparidae fish

Freshly caught fish from Sparidae family: annular seabream, (*Diplodus annularis*), white seabream (*Diplodus sargus*), gilthead seabream (*Sparus aurata*), sand steenbras

(*Lithognathus mormyrus*) and salema (*Sarpa salpa*) were bought from local fish market (Sfax, Tunisia), placed on ice and transported directly to the laboratory. Fresh pyloric caeca from each species were removed after dissection and immediately used for total RNA extractions.

2.2. Reagents

Bacterial cultures were routinely maintained on Luria–Bertani (LB) medium (0.5% yeast extract, 0.5% NaCl, 1% tryptone), with the appropriate antibiotic selection. The different substrates used in this study; 1,2-dilauroyl-*sn*-glycero-3-phosphocholine (DLPC), 1,2-dilauroyl-*sn*-glycero-3-phosphoethanolamine (DLPE); egg yolk phosphatidylcholine (Egg-PC); 1,2-dilauroyl-*sn*-glycero-3-phospho-glycerol (DLPG), 1,2-dilauroyl-*sn*-glycero-3-phosphoserine (DLPS), bovine serum albumin (BSA) and sodium deoxycholate (NaDOC) were purchased from Sigma-Aldrich (Saint-Quentin Fallavier, France). PCR Purification Kit, DNA Gel Extraction Kit, restriction enzymes and T4 DNA ligase were purchased from New England *Biolabs* and were used according to the manufacturers' protocols. Chemicals were obtained from different commercial sources: urea and L-cysteine were from Sigma-Aldrich (Saint-Quentin Fallavier, France). Nickel affinity gel was obtained from Bio-Rad, Isopropyl β-D-1-thiogalactopyranoside (IPTG) and Kanamycin were obtained from Invitrogen (France).

2.3. Strains and plasmids

E.coli Top 10 and BL21 (DE3) strains (Life technologies, France) were used for the cloning of Sparidae PLA_2 genes and for the expression of $AsPLA_2$, respectively. Genes coding for Sparidae PLA_2 were cloned into pCR®-Blunt II-TOPO®vector and then sequenced. For enzyme expression, the genes were cloned into the pET-28b vector in *NcoI* and *NotI* sites allowing the fusion of 6-His tag at the C-terminus.

Searching for mammalian and venom $sPLA_2$ homologs in genomic databases led us to identify a cDNA sequence from: *Pagrus major* a Sparidae species, containing a possible complete open reading frame encoding for a $sPLA_2$ This sequence was used to build primers

and then to amplify, by RT-PCR, cDNA from various Sparidae species encoding for group IB $sPLA_2$ (Table 1).

2.4. Molecular cloning of Sparidae PLA_2

Total RNA was isolated from Sparidae fish's pyloric caeca by using Trizol reagent [14]. 2 µg of total RNA were used as a template for cDNA synthesis using superscript II reverse transcriptase (Invitrogen, USA) following the manufacturer's protocol. cDNA was synthesized using oligonucleotide GACTCGAGTCGACATCGATTTTTTTTTTTTTTTT, as a primer for reverse transcriptase, therefore 3' RACE was subsequently carried out using the adaptor oligonucleotide GACTCGAGTCGACATCGA and the forward primer deduced from the peptide signal of a precursor of *Pagrus major* $sPLA_2$ (GenBank accession number AB009286.1). The PCR mixture contained 10 µM of primers and 10 µM of each deoxynucleoside triphosphate in a final volume of 20 µL. PCR was performed with high-fidelity Phusion DNA polymerase (New England *Biolabs*) under the following conditions: preheating to 98°C for 30 s, then 35 cycles of denaturation at 98°C for 10 s, annealing at 55°C for 30 s, and extension at 72°C for 30 s, followed by final extension at 72°C for 5 min. The PCR product (380 bp) was isolated and ligated into the *EcoRI*, dephosphorylated pCR®-Blunt II-TOPO® Vector, according to the manufacturer's protocol (Invitrogen). Top10 *E. coli* cells were transformed with the ligation mixture. The presence of the appropriated insert was verified by colony PCR and restriction analysis. The sequencing reactions were analyzed with the DNA sequencer ABI PRISM 3100/3100-Avant Genetic Analyzer (California, USA).

The sequencing was performed three times, using the recombinant vector containing *$AsPLA_2$* as template with M13 promoter primers (Invitrogen). The nucleotide sequences of mature $sPLA_2$ from five Sparidae fishes: $AsPLA_2$, gilthead seabream PLA_2 ($GhPLA_2$), saupe PLA_2 ($SpPLA_2$), white seabream ($WsPLA_2$) and sand steenbras ($SsPLA_2$) determined in this

study, were deposited in the GenBank database under accession numbers **KU199228, KU199229, KU199230, KU199231, KU199232**, respectively.

2.5. Protein sequence alignment and phylogenetic analysis

The reading frames of the sequenced cDNAs were translated using EXPASY program and the deduced Sparidae PLA_2 amino-acid sequences were compared with the existing sequences in the NCBI Protein Database using the BLASTP algorithm. The amino-acid sequences of all the Sparidae $sPLA_2$ were aligned and analyzed for the conserved regulatory and catalytically important motifs, employing BioEdit v.7.2.5 method [15]. The deduced amino-acid sequence of $AsPLA_2$ was used as a template to identify homologous $sPLA_2$ sequences in PSI-BLAST researches in the NCBI Protein Database. Forty three homologous group-IB $sPLA_2$ sequences from different mammals, birds, reptiles and fish and insects, were used for multiple sequences alignment using BioEdit v.7.2.5 and the default settings [15]. The output of BioEdit Multiple Sequence Alignment was color coded according to their identity. The amino-acid sequences of $sPLA_2$ phylogenetic trees, conducted in Molecular Evolutionary Genetics Analysis MEGA6, using the Maximum Parsimony method [16]. The robustness of branches was assessed by bootstrap analysis of 100 replicates [17]. All positions containing gaps and missing data were eliminated.

2.6. Recombinant expression of $AsPLA_2$

The cDNA coding for $AsPLA_2$ without its prepropeptide was amplified by PCR using high fidelity KOD polymerase (*New England Biolabs*) and specific primers bearing on their ends the appropriate *NcoI* (5') and *NotI* (3') restriction sites (Table 1). The amplified product was subcloned into the pET-28b vector which had been previously used to express several $sPLA_2$ in *E. coli* [18]. The constructed plasmids were transformed in *E. coli* BL21 (DE3) using the optimized electroporation protocol [19]. The transformed cells were selected on LB agar plates containing 100 µg/mL Kanamycin and streak-purified. The integration of the plasmids

in *E. coli* was confirmed by colony PCR. To determine the time course of the $AsPLA_2$ protein expression, a pilot expression study was carried out. One colony was picked and used to inoculate 3 mL of LB medium containing 50 µg/mL Kanamycin and cultivated at 37°C for 4 h. When optical density (OD) at 600 nm reached 0.8, IPTG was added to the culture in a final concentration of 1 mM and the culture was continued for another 4 h. At various time intervals, an aliquot of the culture (200 µL) was taken and centrifuged at 8000 x g for 5 min. The pellet was dissolved in 0.1 mL of a solution containing 4% SDS, 100 mM Tris-HCl (pH 7), and 0.5 mM β-mercaptoethanol and subjected to SDS-PAGE analysis.

For large-scale expression, the culture (3 mL) was used to inoculate 200 mL fresh LB medium containing 50 µg/mL Kanamycin. When OD_{600} reached 0.8, the protein expression was induced by 1 mM IPTG addition. After induction, the culture was shacked at 37°C for 4 h. Induced cells were harvested by centrifugation at 8000 x g for 10 min and stored at -20°C.

2.7. Refolding and purification of recombinant $AsPLA_2$

For recombinant protein purification, frozen cells were thawed and resuspended in 25mM Tris-HCl buffer (pH 8.0) containing 50 mM NaCl and 20 mM EDTA for 30 min on ice, followed by sonication and centrifugation at 8000 x g for 15 min. The supernatant containing the soluble fraction was removed and the pellet containing the inclusion bodies (unfolded proteins) was resuspended in denaturing buffer containing 25 mM Tris-HCl (pH 8), 5 mM L-cysteine and 8 M urea by stirring overnight at 4°C. The denaturated $AsPLA_2$ was refolded by dialyzing against 2 L of the refolding buffer (25 mM Tris-HCl, pH 8, 5 mM L-cysteine and 0.8 M urea) by mild stirring overnight at 4°C. Any precipitate was removed by filtration through a 0.45 µm filter. Prior to further purification, the urea was removed from the refolded protein by dialyzing twice against 2 L of buffer A (25 mM Tris-HCl (pH 8.0), 10 mM NaCl) overnight at 4°C. Upon complete removal of urea, insoluble proteins were removed by centrifugation at

12 000 x g for 30 min at 4°C and the concentration of refolded protein was estimated using Bradford's procedure [20].

The proteins recovered from the dialysis were loaded onto nickel affinity chromatography column equilibrated with buffer A (25 mM Tris-HCl pH 8.0, 10 mM NaCl). The column was washed with the same buffer. Under these conditions $AsPLA_2$ was bounded to support and eluted with a linear gradient of imidazole (between 0 and 250 mM) at a flow rate of 1 mL/min. The purified fractions were analyzed by SDS-PAGE and stored at -20°C.

2.8. $sPLA_2$ assay

Enzyme activity was measured potentiometrically by titrating the free fatty acids released from mechanically stirred emulsion of phospholipid substrate, using 0.1 N NaOH and a pH-stat apparatus (Metrohm 718 Stat Titrino, Zofingen, Switzerland). Each assay was performed under the optimum conditions, in a thermostated vessel containing 0.5% of phospholipid substrate (Egg-PC) and 30 mL of 150 mM NaCl, 8 mM $CaCl_2$, and 6 mM NaDOC [21]. Under the above assay conditions, one international phospholipase unit (U) corresponds to the release of 1 µmol of fatty acid liberated per minute.

2.9. Monomolecular film technique for kinetic measurements on $sPLA_2$

Kinetic experiments were performed with a KSV-2000 barostat (KSV-Helsinki) and a "zero-order" Teflon trough [22] with two compartments (reaction and reservoir compartment), which were connected to each other by a small surface channel as described previously by Verger and de Haas [22]. The trough was equipped with a mobile Teflon barrier, which was used to compensate for the substrate molecules removed from the film by enzyme hydrolysis, thus maintaining the surface pressure constant. The surface pressure was measured on the reservoir compartment with a Wilhelmy plate (perimeter 3.94 cm) attached to an electromicrobalance, which was connected in turn to a microprocessor programmed to regulate the mobile barrier movement. The reactions were performed at room temperature. The aqueous

subphase contained 10 mM Tris-HCl (pH 8), 150 mM NaCl, 21 mM $CaCl_2$, and 1 mM EDTA with all PLA_2 assays. The enzyme solution, at final concentration of 20 nM, was injected into the subphase of the reaction compartment only when the 1,2-dilauroyl-*sn*-glycero-3-phospholipid films covered both compartments. The reaction compartment was stirred at 250 rpm using magnetic stirrers. The reaction compartment has a surface of 120 cm^2 and a volume of 120 mL. The reservoir compartment was 147 mm wide and 249 mm long.

All activity measurements were performed after 20 min of enzyme injection. Activities were expressed as the number of moles of substrate hydrolyzed by unit time (min) and unit of surface (cm^2) of the reaction compartment for an arbitrary $sPLA_2$ concentration of 1 M.

2.10. Protein quantification and gel electrophoresis

Protein concentrations were determined by using Bradford's procedure [20], using BSA ($E^{1\%}_{1\ cm}$=6.7) as the standard. To estimate the relative molecular mass of the protein, the histidine-tagged $sPLA_2$ fusion protein was analyzed by SDS-PAGE, as reported by Laemmli [23], using 15% polyacrylamide gel under reducing conditions. Native PAGE was performed according to the same procedure except that the sample was prepared without adding SDS and reducing agent and not heated. Protein bands were stained with 0.25% of Coomassie brilliant blue R-250. For the zymographic determination of $sPLA_2$ activity, after the electrophoretic separation of the enzyme preparation on native PAGE, the enzyme activity was detected by incubating the native gel in 6 mM NaDOC, 0.3 mM phenol red as a pH indicator, 150 mM NaCl, 8 mM $CaCl_2$ and 0.1% PC for 60 min at 50°C and pH 8.5 [24]. Protein bands with $sPLA_2$ activity became visible as clear spots.

2.11. Mass spectrometry and NH_2-terminal sequence analysis

MALDI-TOF analysis of $sPLA_2$ were carried out on an Applied Biosystems voyager DE-ROMass spectrometer in linear mode with sinapinic acid as a matrix and using external or internal calibration. In most cases, samples were desalted by purification on Zip-Tip C18

microcolumns (Millipore). The $sPLA_2$was eluted with an H_2O/acetonitrile/trifluoroacetic acid solution (20/80/0.1, v/v/v).

To determine the N-terminal amino acid sequence, the purified $AsPLA_2$ analyzed by SDS-PAGE, was electrophoretically transferred to a polyvinylidene difluoride (PVDF) membrane. The blotted PVDF membrane was stained with 0.1% (w/v) Coomassie brilliant blue R-250 containing 1% acetic acid and 40% methanol. After washing with methanol, the region containing the phospholipase band was cut off from the membrane. The N-terminal amino acid sequence of transferred protein was determined by the Edman's degradation method on an Applied Biosystems Protein Sequencer Procise 492 equipped with 140 C HPLC systems [25].

2.12. Protein modeling and molecular docking

The construction of theoretical three dimensional (3D) models relies on the available structural data from the Protein Data Bank (PDB) repository by using the homology modeling method implemented in MODELLER package [26]. The sequence of $AsPLA_2$ and $WsPLA_2$ shares high aminoacid identity reaching 96%. For such reason we applied comparative modeling only for $AsPLA_2$ and the $WsPLA_2$ model was obtained by an *in silico* mutation. A BLAST homology search was applied over the sequences of PDB to identify a suitable template. The sequence of the template and the target protein were then processed using the pairwise alignment method of Needleman–Wunsch implemented in EMBOSS package [27]. The alignment was used for model building by MODELLER. Several considerations were instructed to the input python script used for the modeling as special restraints, namely the conservation of the geometry of the catalytic dyad and the secondary structure of the beta wing segment where the beta sheet is formed between the 75-79th and the 82-86th residue segment. Two calcium ions were also included in the model. Twenty models were generated using different random seeds which were evaluated with the DOPE score to assess their overall relative quality. Fully automated docking methods accuracy depends on multiple system

dependent parameters and considerations and might not be guaranteed in fully automated protocols. For such a reason, we used a manual procedure in which we take in account the available knowledge about the catalytic process of homologous $sPLA_2$ protein types in order to get a reasonable complex model between 1-palmitoyl-2-oleoyl-*sn*-glycero-3-phosphocholine (POPC), 1-palmitoyl-2-oleoyl-*sn*-glycero-3-phospho-glycerol (POPG) ligand types and the studied enzymes while considering the compatibility with the Gromos 53a6force field. We found the structure of the bee venom $sPLA_2$ co-crystallized with 1-*O*-octyl-2-heptylphosphonyl-*sn*-glycero-3-phosphoethanolamine (OHGPA), an analogue for POPC and POPG (**PDB code 1POC**). We first made a structural alignment between the two amino acids of the catalytic dyad His48 and Asp49 to their equivalent residues in the bee venom $sPLA_2$, His34 and Asp35. The resulting 3D transformation matrix was then used to reassign the coordinates of the OHGPA in such manner to fit in the interaction site of $AsPLA_2$ and $WsPLA_2$. The non-identical chemical groups from OHGPA were replaced by their corresponding counterparts in POPC and POPG to build its topology inside the catalytic binding site of the protein. To remove any residual steric clashes between the atoms of the ligand and the $sPLA_2$ protein, we used energy minimization method where the atoms of the protein and the head group of POPC were restrained followed by another cycle where only the heavy atoms of the enzyme are kept fixed.

2.13. Molecular dynamics simulation:

A simulation of 10 ns was achieved for the complexes of POPC/$AsPLA_2$ and POPG/$AsPLA_2$ using Gromacs 5.1 package [27]. The Gromos 53a6 force field parameters were assigned to all the atoms in the system including the ligand implemented from the lipid parameters set. The complex was first solvated with SPC water type in an octahedron box using a 12 Å cutoff between any solute atoms and the edge of the box. An appropriate number of counter ions were added to neutralize the net charge of the system. Before running the molecular

dynamics phase, energy minimization was used to remove the steric clashes resulting from the manual docking of the ligand to the catalytic binding site of PLA_2. At first a position restraints were applied on the protein atoms and the head group atoms of the ligand to preserve the ideal atomic arrangement of the catalysis. A first, 1000 steps of steepest decent energy minimization of was applied after which all the position restraining forces were removed and another 200 steps of conjugate gradient minimization was applied. The molecular dynamics simulation was conducted under the Particle Mesh Ewald approximation and a finite non bonded cutoff of 12 Å. The LINCS algorithm was applied to constraint the hydrogen atoms bonds which allow us to use 2fs time step for running the dynamics. To equilibrate the system two NVT runs were applied. We remove the restraining forces and continue for an additional 20 ps until the system reach the desired temperature. The simulation was then continued for 100 ps in the NPT ensemble using Parrinello-Rahman pressure Barostat with a coupling time of 2 ps [28]. The production run for 30 ns was conducted after the correct pressure was attained. Snapshots were saved every 100 ps and analyzed with the build in tool provided in Gromacs package.

3. Results and discussion

3.1. Analysis of Sparidae sPLA$_2$ sequences

Sparidae PLA$_2$ cDNAs included a 450 bp open reading frame that encoded a prepropeptide of 23 amino acids, followed by a mature protein of 126 amino acids (Fig. 1A). The alignment of aminoacid sequences for mature Sparidae sPLA$_2$ showed that they shared high identity ranging from 80 to 95%. Multiple sequence alignment of AsPLA$_2$, human pancreatic sPLA$_2$ (HuPLA$_2$) and porcine pancreatic sPLA$_2$ (PPLA$_2$) is shown in Fig. 1B. AsPLA$_2$ shares 45% and 51% aminoacid identities with HuPLA$_2$ and PPLA$_2$, respectively. Furthermore, Sparidae sPLA$_2$ shares about 33%, 35.6%, and 37.4% identity with chicken PLA$_2$-IIA, human PLA$_2$-IIA and human PLA$_2$-GV, respectively (Data not shown).

The alignment of the deduced aminoacid sequence of AsPLA$_2$ with orthologous sPLA$_2$ from mammalian species (Fig. 1B), as well as the analysis of the conserved domains, revealed that AsPLA$_2$ has conserved motifs typical in other pancreatic sPLA$_2$. The phospholipase consensus motif with the catalytic (His48, Asp49) dyad is fully conserved among all studied sPLA$_2$ (Fig. 1B). AsPLA$_2$ is characterized by an N-terminal pro-peptide whose proteolytic removal gives rise to a functional enzyme. The calcium loop consensus sequences YGCXCGXGG is highly conserved in all sPLA$_2$ sequences (Fig.1B). As shown in Fig. 1B, the 14 cysteine residues involved in disulfide bridges in all known sPLA$_2$-GIB [2,4], are also conserved in Sparidae sPLA$_2$ suggesting the presence of 7 disulfide bridges in its 3D structure, that are postulated to be involved in the stability of sPLA$_2$ [3,29]. Among the conventional sPLA$_2$s, sPLA$_2$-IB is probably the oldest sPLA$_2$ subtype in the animal kingdom [29]. It was established that only sPLA$_2$-GIB and sPLA$_2$-X possessed the Cys11-C77, suggesting that sPLA$_2$-X emerged during the diversification from group I to II sPLA$_2$s [30]. Indeed, using site-directed mutagenesis, it was shown that the disulfide bond Cys11-C77 is most important to the conformational integrity and conformational stability of the bovine pancreatic PLA$_2$ [31]. In addition to the presence of a Cys11-Cys77 disulphide bond, which is group I-specific

disulphide, an interesting property of $AsPLA_2$ is the conserved 5 amino acids (62-66) that constitute an hydrophobic loop so-called the pancreatic loop (Fig. 1B). The $AsPLA_2$ pancreatic loop sequence shows more than 50% of similarity with those of both pancreatic $sPLA_2$. All these relevant features indicate that all sequenced $sPLA_2$ belong to pancreatic family group-IB.

3.2. Phylogenetic analysis of digestive $sPLA_2$

The phylogenetic analysis was conducted using 43 sequences containing 26 pancreatic PLA_2, 13 fish digestive PLA_2 and 4 insect PLA_2s. Phylogenetic analysis of the selected organisms suggests that fish digestive PLA_2s share common evolutionary origin with their homologous from reptiles, birds, mammals and insects. According to the established phylogeny, the new sequences of the six Sparidae PLA_2 were grouped together with those of other fish $sPLA_2$ in one fish digestive $sPLA_2$ gene family with a bootstrap value of 97 % (Fig. 2A). In addition, the cluster of the Sparidae digestive PLA_2s is apparently more similar to the reptile PLA_2s than to those of birds and mammals. (Fig. 2A). In fact, the clades corresponding to mammal and bird pancreatic $sPLA_2$ can clearly be distinguished sharing one common ancestor (Fig. 2A). Furthermore, the maximum parsimony phylogenetic tree (Fig. 2B) may be helpful to understand the mechanisms of evolutionary relationships between different Sparidae species and other marine fish. In fact, $sPLA_2$s of the seabass *(Dicentrarchus labrax)* followed by that of the Atlantic salmon *(Salmo salar)* are likely to be the closest species to the common ancestor of the studied Sparidae fish enzymes (Fig. 2B). Among Sparidae $sPLA_2$, the red seabream PLA_2 seems to be the closest to the common ancestor. Indeed, the most recent common ancestor of insects is close to that of fish, according to the phylogenetic tree.

3.3. Recombinant expression and purification of $AsPLA_2$

To accomplish the expression and purification of the recombinant $AsPLA_2$, the protein was obtained by overexpression of the *$AsPLA_2$*-pEt28B in *E. coli* BL21 (DE3) cells. As shown in Fig. 3A (lanes 3-5), a band of expected size (about 15 kDa) was found in the precipitate as inclusion bodies after centrifugation of the disrupted cells. Consequently, the isolation of these

inclusion bodies was the first step in the purification process of the recombinant protein. After cell lysis, the inclusion bodies were separated by centrifugation and dissolved in the denaturing buffer containing urea as chaotropic agents. The denatured $AsPLA_2$ was refolded following the different steps listed in Material and Methods. The dialyzed supernatant containing the $AsPLA_2$ activity was purified by affinity chromatography on Ni-agarose column (Fig 3B). The His-tag expression system is widely used for the affinity purification of recombinant enzymes due to its low molecular weight and because it do not affect protein structure and function [32]. The effect of His-tag extension on recombinant proteins is a matter of debate. Some studies report an effect of His-tag on other proteins such as dehydrogenases [32] , but it was shown in the particular case of some lipases [33] and galactophospholipase [34] that His-tag extension had little effects on the biochemical properties of the enzyme. The active $AsPLA_2$ was eluted between 25 and 100 mM imidazole (Fig. 3B). The active fractions were pooled and analyzed by SDS-PAGE (Fig. 3C). A single protein band with an apparent molecular mass of about 15 kDa, corresponding to the $AsPLA_2$ was observed. The $sPLA_2$ activity of this protein band was confirmed by a zymogram assay under native conditions (Fig. 3D). Only a single band with enzymatic activity corresponding to pure $AsPLA_2$ was revealed. The MALDI-TOF mass spectrometry analysis of the recombinant $AsPLA_2$ revealed a major peak at 15,396.78 kDa (Fig. 3E). This value is close to that calculated from the primary sequence of the mature protein (15,516.09 kDa) with four aminoacid (A-A-A-L-E) before the 6xHis-tag sequence at the C-terminal. The difference between the theoretical and the practical mass can be explained by the loss of the C-terminal histidine probably due to proteolysis during/after purification. Analysis of the N-terminal sequence of the recombinant $AsPLA_2$ was performed by Edman degradation in an automated protein sequencer and found to be A-L-N-Q-F-R-E-M. The purification flow sheet is shown in Table 2. Starting with 26 mg of proteins after inclusion bodies solubilization, around 13 mg of pure $AsPLA_2$ was obtained. The enzyme has a specific activity of 400 U/mg

on Egg-PC used as substrate. It is worth noticing that the specific activity of the recombinant $AsPLA_2$ is higher than that of *Asterina pectinifera s*PLA_2 (119 U/mg) [35]. Comparable specific activities were reported for dromedary (326 U/mg) and chicken (400 U/mg) pancreatic $sPLA_2$s [6, 36].

3.4. Enzymatic properties of the purified $AsPLA_2$

3.4.1. Effects of pH on $AsPLA_2$ activity and stability

The purified enzyme was mostly active between pH 8 and 9 with an optimum at pH 8,5 (Fig. 4A). The optimum pH value for the recombinant $AsPLA_2$ activity was close to the one described for other $sPLA_2$s from marine species such as green crab [37], marine snail (*Hexaplex trunculus*) [38] and stingray (*Dasyatis pastinaca*) [39]. At pH 8, $AsPLA_2$ activity (400 U/mg) seems to be higher than those of marine invertebrate species PLA_2 (about 40 U/mg for green crab [37] and 180 U/mg for marine snail [38]). In contrast to porcine pancreatic PLA_2, the recombinant $AsPLA_2$ was found to be mostly stable at an alkaline pH ranging from 7.5 to 9 (Fig. 4B). Similar results were reported for stingray, the marine snail and the crab $sPLA_2$s [37-39].

3.4.2. Effects of temperature on $AsPLA_2$ activity and stability

Phospholipase activity was tested at temperatures ranging from 30 to 60°C using homogeneous Egg-PC emulsion as substrate. For the sake of comparison we also report the results for porcine pancreatic phospholipase ($PPLA_2$) in Fig. 4C and 4D. In contrast to all known mammals' pancreatic phospholipases like $PPLA_2$ (Fig. 4C) which display their maximal activity at 37 °C, the maximal $AsPLA_2$ activity was measured at 50°C. The rate velocity of crab phospholipase increased significantly when the temperature passed from 37 to 50°C under optimal assay conditions (0.5% of phospholipid substrate (Egg-PC) and 30 mL of 150 mM NaCl, 10 mM $CaCl_2$, and 8 mM NaDOC). This optimum was similar to that of $sPLA_2$ from the pyloric ceca of starfish [35] and the green crab hepatopancreas [37], and higher than those of

mammalian pancreatic $sPLA_2$, like dromedary [6] and bovine [40], which optimal activity temperature is around 37°C, measured under similar assay conditions. At 50°C, $AsPLA_2$ activity (400U/mg) seems to be higher than those of marine invertebrate species PLA_2 (about 40 U/mg for green crab and 180 U/mg for marine snail [37, 38]).

The $AsPLA_2$ thermo-stability was investigated by preincubation of the enzyme at various temperatures and measuring the residual activity under optimal experimental conditions. Recombinant $AsPLA_2$ retained its maximum activity after incubation for 15 min between 30 and 60°C (Fig. 4D). The $AsPLA_2$ activity decreased significantly upon incubation at a temperature higher than 60°C. This behavior recalls that of *Hexaplex trunculus* $sPLA_2$ [38]. The thermo-activity of $AsPLA_2$ suggested that the enzyme was probably protected at higher temperature by the presence of its substrate [37]. Comparable results were obtained with with green snail digestive PLA_2 and pancreatic PLA_2 for which the presence of the substrate increases the thermostability of the lipolytic enzymes [37,38]. As shown in Fig. 4D, the $PPLA_2$ seems to be less stable than the $AsPLA_2$ in the absence of substrate. Indeed the porcine phospholipase was inactivated at 60°C. However, the sparidae phospholipase continue to display 50% of its maximal activity at the same temperature.

3.4.3. Calcium ions and bile salts dependence

Conventional $sPLA_2$s have a highly conserved Ca^{2+}-binding site [1]. It has been demonstrated that the $sPLA_2$s requires the presence of calcium ions for both catalysis and enzyme binding to the substrate [4,41,42]. The calcium ion is absolutely required for hydrolysis and it stabilizes the transition state by coordinating the conserved carbonyl oxygens of the tyrosine and glycine from the calcium binding loop [1]. In order to investigate the effect of Ca^{2+} on the recombinant $AsPLA_2$ activity, we studied the variation of PC hydrolysis rates by the pure $AsPLA_2$ in the presence of various Ca^{2+} concentrations (Fig. 5A). Our results showed that no $sPLA_2$ activity was observed in the absence of Ca^{2+} and in the presence of a bivalent ion chelator (EDTA). In the absence of calcium chelators, the highest specific activity of purified $AsPLA_2$

was reached at 10 mM $CaCl_2$ (400 $U.mg^{-1}$) (Fig. 5A). These observations corroborate previous findings with bovine [40] and chicken $sPLA_2$-IB [36]. In the presence of 10 mM of $CaCl_2$, the $AsPLA_2$ shows a lower specific activity than the stingray PLA_2 (750 $U.mg^{-1}$) [39] and the dromedary pancreatic PLA_2 (600 $U.mg^{-1}$) [6]. Whereas a higher activity has been observed for $AsPLA_2$ than invertebrates (180 $U.mg^{-1}$for marine snail).

Several studies have provided evidence that bile salts are tensioactive agents ensuring in their micellar form, the dispersion of the lipolytic hydrolysis products [43]. In this study, we measured the recombinant $AsPLA_2$ activity at pH 8.5 and at 50°C using Egg-PC as a substrate in the presence of increasing concentrations of bile salts (NaDOC). As shown in Fig. 5B, bile salts were required for $AsPLA_2$ activity. In fact, the recombinant enzyme activity increased to reach its maximum in the presence of 10 mM NaDOC. These observations are in line with the fact that $sPLA_2$ from various origins are activated by bile salts [6, 39].

3.4.4. Substrate specificity of $AsPLA_2$ toward various phospholipids and surface pressures

In order to investigate the ability of the recombinant $AsPLA_2$ to penetrate and to hydrolyze phospholipids monolayer films, the hydrolysis reactions towards zwitterionic phospholipids: DLPC and DLPE and negatively charged phospholipids: DLPG and DLPS by $AsPLA_2$ were performed. Fig. 6 illustrates the activity-surface pressure profiles obtained with the four phospholipids using pure recombinant enzyme. $AsPLA_2$ was found to be active on all phospholipids tested at different surface pressures. It is clear that the $AsPLA_2$ activity measured on DLPG films was the highest as compared to those measured on the other phospholipids (Fig. 6). These results are in agreement with the fact that DLPG is considered to be the best substrate for the most known $sPLA_2$ [1,43]. The optimum activity of $AsPLA_2$ on DLPG (30 $moles.cm^{-2}.min^{-1}.M^{-1}$) was obtained at a surface pressure of 10 $mN.m^{-1}$. Except the DLPS, the activity-surface pressure profiles obtained with the other phospholipids show a bell shaped curves with a characteristic optimal surface pressure values between 10 and 20 $mN.m^{-1}$ (Fig. 6). However,

the hydrolysis rate of DLPS was negligible at low surface pressure and increased continuously until 30 $mN.m^{-1}$.

3.5. Structural characterization of $AsPLA_2$

The functional properties of the purified $AsPLA_2$ and its potential in biological applications thrust us to establish the 3D structure models of fish $sPLA_2$s.

3.5.1. 3D model of $AsPLA_2$

The 3D structure of the *Sus scrofa* phospholipase A_2 (PDB code 4P2P) was used as a template to build models for the recombinant $AsPLA_2$ and $WsPLA_2$ using the program MODELLER. The root mean squared deviation (RMSD) involving α-carbons between the initial and the optimized models were 0.8 Å for both $sPLA_2$s. The sequence identity between the template and the target sequences is at 57% sitting above the twilight zone. Ramachandran assessment quality plot showed that all the (phi, psi) dihedral angles are either situated in the highly favorable zones (98%) or in the allowed regions (2%). The $AsPLA_2$ present the hallmark of pancreatic $sPLA_2$ with a globular folding (Fig. 7A). A typical fold consisting of four major helices constitutes the main core of the protein packed to each other with the help of three disulfide bonds. Helix Alpha 2 is connected to the catalytic calcium coordinating loop with another disulfide bond between C29 and C45. A double strand β sheet composed by segments 75-78 and 83-86 form the β wing structure of $sPLA_2$ (Fig. 7A, 7B). The latter is reticulated to the alpha helical core of the protein with two disulfide bonds C11-C77 and C86-C98. Residues Y28, G30 and G32 are coordinating the calcium ion of the catalytic dyad, while F27, E94 and D71 bind the second calcium ion (Fig. 7B). It is well known that increasing hydrophobicity of the binding site usually improves the activity of lipolytic enzymes by enhancing affinity to the lipophilic substrate. The turkey pancreatic lipase was found to withstand high interfacial tension in the absence of surfactants and to highly active in these conditions, unlike the Human lipase. This was explained by a higher hydrophobic plateau in the substrate recognition site [44].

Furthermore, fixing a hydrophobic alkyl chain directed to the interface, on a cysteine residue, increased highly the catalytic activity of the turkey pancreatic lipase [44]. A similar behavior was also reported for the human PLA_2. Mutation of Trp31 on the putative interfacial binding site of human group V $sPLA_2$ to alanine reduces the activity of this enzyme on PC vesicles and reduces binding to PC-coated polymer beads [45]. Furthermore, replacement of V3 of human group IIA phospholipase A_2 by tryptophan increases the specific activity of this enzyme on PC vesicles by at least 2 orders of magnitude [46]. These results show that non electrostatic effects can be important for modulating interfacial binding of $sPLA_2$. To bring more explanation for the higher activity of $AsPLA_2$, a determination of the hydrophobic cluster on the surface areas of the binding site was required. Compared to the $HuPLA_2$ (P04054), the $WsPLA_2$ and $AsPLA_2$ share 55% of amino acid identical residues (68% of homologous residues) (see Fig. 7B). As compared to $HuPLA_2$, the $AsPLA_2$ and $WsPLA_2$ display a higher hydrophobic surface in the membrane interacting interface. This was mainly observed for the loop connecting the α2 major helix to the β strand of the β wing in its N-terminal side (Fig. 7). The loop contains exposed apolar amino acids W62, I64, L65 equivalent to K62, L64 an L65 in the $HuPLA_2$ structure (Fig. 7A). F72 residue is also substituted with polar amino acid T72 in the $HuPLA_2$. In both $WsPLA_2$ and $AsPLA_2$ structures, the total apolar surface areas are around 4731 and 4700 Å², respectively. These values are higher than the corresponding surface in $HuPLA_2$ (4265 Å²). The exposed hydrophobic surface suggested to contribute to the substrate binding was higher for the $WsPLA_2$ (1400 Å²), and $AsPLA_2$ (1345 Å²) (Fig. 7B) than that of $HuPLA_2$ (956 Å²) (Fig. 7B). In particular, Y31 and L2 from α1 helix participate in increasing the exposed hydrophobic surface of $WsPLA_2$ and $AsPLA_2$. Altogether, these results are in line with the higher activity towards phospholipids. In fact the specific activities of the $AsPLA_2$ and $HuPLA_2$ assessed on PC vesicles in the same conditions were 400U/mg and 600U/mg, respectively (data not shown).

3.5.2. Molecular docking and dynamic simulation

Analysis of the $AsPLA_2$ structure bound to phospholipids can help us to understand the interaction mode of the substrate once located in the catalytic site [47]. The manual docking of POPC and POPG was achieved based on the crystal structure of the bee venom PLA_2 (Fig. 8A). The inter-atomic contacts with POPC and POPG with the enzyme amino acids were analyzed from the energy minimization refined complexes. The catalytic H48 and D49 constituting the catalytic dyad together with Y69 and Y31 represent the main residues interacting with phosphocholine and phosphoglycerol groups of POPG and POPC respectively. The *sn*-2 carbonyl oxygen is at 2.3 and 2.4 Å from the catalytic calcium ion for POPC and POPG, respectively. The alkyl chain at the *sn*-2 position is partially enclosed in a hydrophobic cleft. The *sn-2* carbon hydrophobic tail is adjusted in a longitudinal orientation relative to the main axis of the interaction binding site for the 1-6 carbons, involving residues F5, Y22 and F108 while the other atoms are stabilized by a set of aromatic amino acids, namely F20 and Y31 from the long loop spanning both H_1 and H_2 helices. The chain at the *sn*-1 position is widely exposed but still interacts with several residues of the $AsPLA_2$ including L2, V18 and F20 for POPG and L2, R6, F20 and H119 for POPC. During the molecular dynamics runs for $AsPLA_2$/POPC and $AsPLA_2$/POPG complexes, the carbonyl group of the s*n*-2 position remains at an average distance of 2.3 Å for both POPG and POPC ligands (Fig. 8A). *Sn*-1 carbon chain is in contrast flexible and shows no apparent stable conformations during the 10 ns. The hydrophobic tail of the alkyl chain is highly exposed to the solvent.

The inventory of hydrogen bonds between POPC/POPG and $AsPLA_2$ revealed a major difference between the two ligands. POPC cannot establish stable hydrogen bonds with the enzyme (Fig. 8A). Interestingly, POPG head group presents however a hydrogen bond with 53% of occupancy established between the hydroxyl groups of the glycerol group and the D49 side chain of the catalytic dyad (Fig. 8A), which probably stabilize much better the POPG ligand in the catalytic dyad. These results would explain the higher activity of $AsPLA_2$ towards

DLPG. These findings are in line with the monolayer kinetics, which shows that $AsPLA_2$ was more active on DLPG than on DLPC monolayer (Fig. 6).

3.5.3. $AsPLA_2$ stability and flexibility

The purified $AsPLA_2$ was found to be active and stable at a wide interval of temperatures (37°C-50°C). The $AsPLA_2$ is more thermo-tolerant than the human $sPLA_2$ which possess the optimal temperature of activity at 37°C in the same conditions used to assess the $AsPLA_2$ activity. The key feature of an enzyme function is the maintenance of a suitable balance between molecular stability and structural flexibility.

In order to explain the thermo-stability of the $AsPLA_2$, we used molecular dynamic simulations that were used to investigate thermo-activity of *Candida antarctica*, *Candida rugosa*, and *Yarrowia lipolytica* lipases [48,49]. Molecular dynamics simulations (30 ns) were carried out for the $AsPLA_2$ model at medium (38°C) and high (51°C) temperatures.

To compare the dynamics features of $AsPLA_2$ to the $HuPLA_2$ enzyme an additional simulation was also made for the latter enzyme at 51°C (324 K).

Analysis of the RMSD evolution during the simulation shows that $AsPLA_2$ complex Cα atom fluctuation converges to the same values especially for the last 6 ns of the simulation. This might indicate that the enzyme behaves similarly at both 38°C (311 K) and 51 °C (324 K) (Fig. 8B).

The root-mean-square fluctuation (RMSF) values in the molecular dynamic simulations are usually considered as a criterion to evaluate the overall flexibility of a system. RMSF values for the Cα atoms were calculated as a function of simulation time (Fig. 8B). The residues forming the alpha helices of the protein are less flexible parts of the $AsPLA_2$ and this is expected since they present a dense hydrogen bond network contributing in the rigidity of the whole structure. The results show that the increase in the temperature does not necessary result in the increase of the local flexibility of all segments. Indeed, the RMSF is more important for

segments including 81-89 and 111-116, at 38 °C (Fig. 8C). On the other hand, the segment 59-65 seems to be more flexible at 51°C. These loops seem therefore to be particularly flexible than the other loops separating the rigid secondary structure elements of the protein. In such case this could be attributed to the redistribution of the dynamics of the local segments [50]. Stabilizing the protein core which holds the catalytic dyad of the enzyme and the ligand binding pocket at both temperatures is consistent with the thermostability of the purified $AsPLA_2$, which was found to be fully active between 37 and 50°C and would explain why $AsPLA_2$ is more active at 50°C.

In comparison to $HuPLA_2$, The flexibility of the $AsPLA_2$ loop 67-70 (Asn-Pro-Tyr-Thr) equivalent to same residues in $HuPLA_2$ is enhanced. This segment contributes to the interaction with the polar head group of POPC ligand including residue Y69. This might help in accommodating the substrate in the active site in such a high temperature.

Concluding remarks and perspectives

This work describes the cloning of genes from Sparidae fish, encoding for matures PLA_2s, which are homologous to pancreatic $sPLA_2$ group IB. The $AsPLA_2$ was over-expressed in *E.coli*, purified and characterized. To further expand the industrial use of enzymes, catalytic and biophysical properties of enzymes, such as catalytic efficiency, substrate specificity, thermoactivity and stability, should be satisfied. Unlike porcine pancreatic phospholipase, $AsPLA_2$ is active and stable at 50°C. The sparidae PLA_2 hydrolyzed egg-yolk PC substrate effectively at alkaline pH with optimum activity of about pH 8.5, and showed a high preference to PG than PE and PC. Our investigation clearly demonstrates that $AsPLA_2$ has similar features to other marine species PLA_2s. The important activities recorded for fish PLA_2 can be related to their ability to recover unsaturated fatty acids localized generally in the sn-2 position of food phospholipids. This would allow an enrichment of fish lipids in unsaturated fatty acids in

general and omega-3 ones in particular. This work allowed the identification of a new candidate with relevant properties for potential industrial applications.

Conflict of interest

Dear Editor,

Please find enclosed a PDF format of our manuscript entitled "Efficient heterologous expression, functional characterization and molecular modeling of annular seabream digestive phospholipase A_2" by Nabil SMICHI et al. for consideration for publication in "Chemistry and Physics of Lipids" as a regular article.

We state on our honor that the manuscript has not been previously published, is not currently submitted for review to any other journal, and will not be submitted elsewhere before a decision is made by this journal. By common consent, all the authors mutually agree for its submission for publication in Chemistry and Physics of Lipids. The authors also agree to transfer the copyright from the authors to the publisher in case of acceptance. The manuscript does contain experiments using animals. The experimental protocols and procedures used in the present work were approved by the Ethics Committee of the University of Sfax (Sfax, Tunisia) for the care and use of laboratory animals.

Sincerely yours,
Dr. Ahmed Fendri

Acknowledgments

We thank Dr. Pascal MANSUELLE for technical assistance with MALDI-TOF spectrometers. This work was supported by the Ministry of higher education and scientific research of Tunisia.

References

[1] E.A. Dennis, J. Cao, Y.H. Hsu, V. Magrioti, G. Kokotos, Phospholipase A2 enzymes: physical structure, biological function, disease implication, chemical inhibition, and therapeutic intervention, Chem. Rev. 111 (2011) 6130–6185.

[2] T.J. Nevalainen, I. Morgado, J.C. Cardoso, Identification of novel phospholipaseA2 group IX members in metazoans, Biochimie 95 (2013) 1534–1543.

[3] R.H. Schaloske, E.A. Dennis, The phospholipase A2 superfamily and its group numbering system, Biochim. Biophys. Acta, 1761 (2006) 1246–1259.

[4] M. Murakami, H. Sato, Y. Miki, K. Yamamoto, and Y. Taketomi. Thematic Review Series: Phospholipases: Central Role in Lipid Signaling and Disease A new era of secreted phospholipase A_2, J. Lipid Res. 56 (2015) 1248–1261.

[5] I. Jridi, I. Catacchio, H. Majdoub, D. Shahbazeddah, M. El Ayeb, M. A. Frassanito, D. Ribatti, L. Borchani, Hemilipin, a novel *Hemiscorpius lepturus* venom heterodimeric phospholipase A2, which inhibits angiogenesis in vitro and in vivo, Toxicon 105 (2015) 34-44.

[6] A. Ben Bacha, S.K. Al-Daihan, H. Mejdoub, Purification, characterization and bactericidal activities of phospholipase A2 from the dromedary intestine, Inter. J. Biol. Macromol. 57 (2013) 156–164.

[7] Y. Fujikawa, M. Shimokawa, F. Satoh, O. Satoh, D. Yoshioka, S. Aida, K. Uematsu, N. Iijima, Ontogeny of gene expression of group IB phospholipase A2 isoforms in the red seabream, *Pagrus* (Chrysophrys) *major*, Comp. Biochem. Physiol. Part A: Mol. Integ. Physiol. 161 (2012) 185–192.

[8] J.L. Zambonino Infante, C.L. Cahu, High dietary lipid levels enhance digestive tract maturation and improve *Dicentrarchus labrax* larval development, J. Nutr. 129 (1999)1195–1200.

[9] J.L. Buchet, Zambonino Infante, C.L. Cahu, Effect of lipid level in a compound diet on the development of red drum (*Sciaenops ocellatus*) larvae, Aquaculture 184 (2000) 339–348.

[10] A. Sæle, P.A. Nordgreen, K. Olsvik, Hamre, Characterization and expression of secretory phospholipase A2 group IB during ontogeny of Atlantic cod (*Gadus morhua*), Br. J. Nutr. 105 (2011) 228–237.

[11] C. Castro, A. Jiménez, F. Coutinho, P. Pousão-Ferreira, T.M. Brandão, A. Oliva-Teles, H. Peres, Digestive enzymes of meagre (*Argyrosomus regius*) and white seabream (*Diplodus*

sargus). Effects of dietary brewer's spent yeast supplementation, Aquaculture 416 (2013) 322–327.

[12] T.S.C. Roy, A. Gopalakrishnan, brief communications Identification of groupers based on pyloric caeca differentiation, J Fish Biol. 79 (2011), 1334 – 1339.

[13] S. Uchiyama, Y. Fujikawa, K. Uematsu, H. Matsuda, S. Aida, N. Iijima, Localization of group IB phospholipase A(2) isoform in the gills of the red sea bream, Pagrus (Chrysophrys) major, Comp Biochem Physiol B Biochem Mol Biol. 132 (2002), 671-83.

[14] J. Sambrook, E.F. Fritsch, T. Maniatis, Molecular Cloning: A Laboratory Manual. Second edition (1626 pp). Cold Spring Harbor Laboratory Press, Cold Spring Harbor, NY (1989).

[15] T.A. Hall, "BioEdit" a user friendly biological sequence alignment editor and analysis program for windows 95/98/NT, Nucleic acids symposium Series 41 (1999) 95-98.

[16] K. Tamura, G. Stecher, D. Peterson, A. Filipski, S. Kumar, MEGA6: Molecular Evolutionary Genetics Analysis version 6.0, Mol. Biol. Evol. 30 (2013) 2725-2729.

[17] K. Tamura, F.U. Battistuzzi, P. Billing-Ross, O. Murillo, A. Filipski, S. Kumar, Estimating Divergence Times in Large Molecular Phylogenies, Proc. Nat. Aca. Sc. 109 (2012) 19333-19338.

[18] D. Cavazzini, F. Meschi, R. Corsini, A. Bolchi, G.L. Rossi, O. Einsle, S. Ottonello, Autoproteolytic Activation of a Symbiosis-Regulated Truffle Phospholipase A2, J Biol. Chem. 288 (2013) 1533–1547.

[19] S. Wu, G.J. Letchworth. High efficiency transformation by electroporation of *Pichia pastoris* pretreated with lithium acetate and dithiothreitol, Biotechniques 36 (2004) 152-154.

[20] M.M. Bradford, A rapid and sensitive method for the quantitation of microgram quantities of protein utilizing the principle of protein-dye binding, Anal. Biochem. 72 (1976) 248–254.

[21] A. Abousalham, R. Verger, Egg yolk lipoproteins as substrates for lipases, Biochem Biophys Acta. 1485 (2000) 56-62.

[22] F. Pattus, A.J. Slotboom, G.H. de Haas, Regulation of phospholipase A2 activity by the lipid–water interface: a monolayer approach, Biochemistry 18 (13) (1979) 2691–2697.

[23] U.K. Laemmli, Cleavage of structural proteins during the assembly of the head of bacteriophage T4, Nature 227 (1970) 680–685.

[24] A.L. Araujo, F. Radavanyi, Determination of phospholipase A_2 activity by a colorimetric assay using a pH indicator, Toxicon, 25 (1987) 1181–1187.

[25] R.M. Hewick, M.W. Hunkapiller, L.E. Hood, A gas-liquid solid phase peptide and protein sequenator, J. Biol.Chem. 256 (1981) 7990–7997.

[26] P. Rice, I. Longden, A. Bleasby, EMBOSS: the European Molecular Biology Open Software Suite, Trends Genet. 16 (2000) 276-277.

[27] W.F. Van Gunsteren, S.R. Billeter, A.A. Eising, P.H. Hunenberger and P. Kruger Biomolecular simulation: the GROMOS96 manual and Applied Microbiol. Biotechnol user guide, vdf Hochschulverlag AG an der ETH Zurich and BIOMOS b.v, Zurich, Switzerland, (1996) 1–1042.

[28] M. Parrinello, A. Rahman, Polymorphic transitions in single crystals: A new molecular dynamics method, J. Phys. 52 (1981) 7182-7190.

[29] M. Murakami, Y. Taketomi, Y. Miki, H. Sato, T. Hirabayashi, K. Yamamoto. Recent progress in phospholipase A2 research: From cells to animals to humans, Prog. Lipid Res. 50 (2011) 152–192.

[30] L. Cupillard, K. Koumanov, M.G. Mattei, M. Lazdunski, G. Lambeau. Cloning, chromosomal mapping, and expression of a novel human secretory phospholipase A_2, J. Biol. Chem. 272 (1997) 15745-15752.

[31] H. Zhu, C.M. Dupureur, X. Zhang, M.D. Tsai. Phospholipase A_2 engineering. The roles of disulfide bonds in structure, conformational stability, and catalytic function, Biochemistry 34 (1995)15307-14.

[32] Y.J. Yeon, H.J. Park, H.Y. Park, Y.J. Yoo. Effect of His-tag Location on the Catalytic Activity of 3-hydroxybutyrate Dehydrogenase. Biotechnol. Bioprocess Eng. 19 (2014) 798-802.

[33] H. Horchani, A. Fendri, H. Louati, A. Sayari, Y. Gargouri, R. Verger. Purification, biochemical and kinetic properties of recombinant Staphylococcus aureus lipase. Methods Mol. Biol. 861 (2012) 267-82.

[34] R. Jallouli, MB. Ali, M. Charfeddine, R. Gargouri-Bouzid, Y. Gargouri, S. Bezzine. Heterologous overexpression and biochemical characterization of the (galactophospho)lipase from *Fusarium solani* in *Pichia pastoris* that is expressed in planta, Int J Biol Macromol. 84 (2016) 94-100.

[35] H. Kishimura, K. Hayashi, Isolation and characteristics of phospholipase A2 from the pyloric ceca of the starfish *Asterina pectinifera*, Comp. Biochem. Physiol. B. Biochem. Mol. Biol. 124 (1999) 483–488.

[36] A. Karray, F. Frikha, A. Ben Bacha, Y. Ben Ali, Y. Gargouri, S. Bezzine, Biochemical and molecular characterization of purified chicken pancreatic phospholipase A2, FEBS J, 276 (2009) 4545-4554.

[37] S. Cherif, Y. Gargouri, Thermoactivity and effects of organic solvents on digestive lipase from hepatopancreas of the green crab, Food Chem. 116 (2009) 82–86.

[38] Z. Zarai, A. Ben Bacha, H. Horchani, S. Bezzine, N. Zouari, Y. Gargouri, Hafedh Mejdoub, A novel hepatopancreatic phospholipase A2 from *Hexaplex trunculus* with digestive and toxic activities, Archives. Biochem. Biophys. 494 (2010) 121–129.

[39] Ben Bacha, I. Abid, H. Horchani, H. Mejdoub, Enzymatic properties of stingray *Dasyatis pastinaca* group V, IIA and IB phospholipases A (2): a comparative study, Int. J. Biol Macromol. 62 (2013) 537-42.

[40] M. Teke, A. Telefoncu, Purification of bovine pancreatic phospholipase A2 by an affinity ultrafiltration technique, Sep. Pur. Tech. 63 (2008) 716‑720.

[41] A.G. Singer, F. Ghomashchi, C. Le Calvez, J. Bollinger, S. Bezzine, M. Rouault, M. Sadilek, E. Nguyen, M. Lazdunski, G. Lambeau, M.H. Gelb, Interfacial kinetic and binding properties of the complete set of human and mouse groups I, II, V, X, and XII secreted phospholipases A2, J. Biol.Chem. 277 (2002) 48535–48549.

[42] M. Murakami, Y. Taketomi, H. Sato and K. Yamamoto, Secreted phospholipase A2 revisited, J. Biochem. 150 (2011) 233–25.

[43] D.L. Scott, Z. Otwinowski, M.H. Gelb, P.B. Sigler, Crystal structure of bee venom phospholipase A2 in a complex with a transition-state analogue, Science 250 (1990) 1563-1566.

[44] A. Fendri, F. Frikha, H. Louati, M. Bou Ali, H. Gargouri, Y. Gargouri, N. Miled, Cloning and molecular modeling of a thermostable carboxylesterase from the chicken uropygial glands, J. Mol. Graph. Model. 56 (2015) 1–9.

[45] S.K. Han, K.P. Kim, R. Koduri, L. Bittova, N.M. Munoz, A.R. Leff, D.C. Wilton, M.H. Gelb, W. Cho, Roles of Trp31 in high membrane binding and proinflammatory activity of human group V phospholipase A2, J. Biol. Chem. 274 (1999)11881–11888.

[46] B.Z.Yu, O.G. Berg, M.K. Jain, The divalent cation is obligatory for the binding of ligands to the catalytic site of secreted phospholipase A2, Biochemistry, 32(1993) 6485–6492.

[47] C.L. Wee, K. Balali-Mood, D. Gavaghan, M.S. Sansom, The interaction of phospholipase A2 with a phospholipid bilayer: coarse-grained molecular dynamics simulations, Biophys. J. 95 (2008) 1649-57.

[48] Y. Wang, D.Q. Wei, J.F. Wang, Molecular dynamics studies on T1 lipase: insight into a double-flap mechanism, J. Chem. Inf. Model. 50 (2010) 875–878.

[49] F. Bordes, S. Barbe, P. Escalier, L. Mourey, I. André, A. Marty, S. Tranier, Exploring the conformational states and rearrangements of *Yarrowia lipolytica* Lipase, Biophys. J. 99 (2010) 2225–2234.

[50] R. Grünberg, M. Nilges, J. Leckner. Flexibility and conformational entropy in protein-protein binding, Structure 14 (2006) 683-693.

Legend of figures

Fig.1. Multiple sequence alignment of Sparidae PLA_2. **(A)** Alignment of the amino acid sequences of the five Sparidae PLA_2: $AsPLA_2$, $SpPLA_2$, $GhPLA_2$, $SsPLA_2$ and $WsPLA_2$. Identical residues are colored in purple. Boxes in light shaded indicate positions at which the residues were different in the five PLA_2. Numbers indicate residues positions. Homology alignment was performed using the software BioEdit version 7.2.5 [15]. **(B)** Alignment of the aminoacid sequences of $AsPLA_2$ and $HuPLA_2$. Boxes in grey light shaded indicate positions at which the residues are different. The closed arrows indicate the position of Asp and His residues which form the catalytic dyad. The dashes represent gaps found upon sequences alignment.

Fig.2. Phylogenetic relationship of sparidae PLA_2 with pancreatic ones. **(A)** Unrooted phylogenetic tree based on the alignment of the whole phospholipase sequences. The evolutionary history was inferred using the Maximum Parsimony method. A genetic distance scale is shown. The number of times a clade (sequences common to a node or branch) occurred in the bootstrap replicates are shown. Only replicate values of 70 or more, which are significant, are shown. One hundred bootstrap replicates were performed in each case. The analysis involved 43 amino acid sequences. There were a total of 105 positions in the final dataset. **(B)** Neighbor joining phylogenetic tree of five amino acid digestive phospholipase sequences of different fish species (Time tree): Annular seabream digestive Phospholipase ($AsPLA_2$), Salema PL ($SpLA_2$), Gilthead seabream PL ($GhPLA_2$); Stripped seabream PL($SsPLA_2$), White seabream PL ($WsPLA_2$) and five other fish's phospholipases. The evolutionary history was inferred using the Neighbor-joining method [16]. Divergence times for all branching points in the topology were calculated with the RelTime method [17] using the branch lengths contained in the inferred tree. All positions containing gaps and missing data were eliminated. Evolutionary analyses were conducted in MEGA6 [16].

Fig.3. Purification of the recombinant $AsPLA_2$ expressed in *E. coli* (DE3). **(A)** SDS–PAGE analysis of the protein fractions of the bacteria expressing the $AsPLA_2$ fusion protein. Lane M, molecular weight marker; lane 1, positive control (*E. coli* clone expressing a 20 kDa protein); lane 2, (negative control (*E. coli* transformed by empty pET-28b), lanes 3-5, induced cells transformed by *AsPLA*$_2$- pET-28b. (**B**) Chromatogram profile of recombinant $AsPL_2$ pooled from Nickel gel column, as indicated in the Materials and Methods section. **(C)** SDS–PAGE (15% acrylamide) analysis of fractions showing $AsPLA_2$ activity. The gel was stained with Coomassie brilliant blue. Lane 1, molecular mass markers; lane 2 and 3, pooled fractions from affinity column. **(D)** Zymogram analysis of pure $AsPLA_2$. **(E)** Pure $AsPLA_2$ analyzed by MALDI-TOF mass spectrometry analysis as described under "Materials and Methods".

Fig.4. Effects of temperature and pH, calcium on $AsPLA_2$ activity and stability. **(A)** Effect of pH on $AsPLA_2$ activity. $AsPLA_2$ activity was measured at 50 °C at different pH values. **(B)** Effect of pH on $AsPLA_2$ stability. pH stability was analyzed after pre-incubating the pure enzyme for 4 h in different buffer solutions at various pH ranging from 3 to 11 and the remaining phospholipase activity was measured at standard conditions. **(C)** Effect of temperature on $AsPLA_2$ activity. PLA_2 were tested for activity at pH 8.5 at various temperatures. **(D)** Effect of temperature on $AsPLA_2$ stability. For temperature stability the pure enzyme was pre-incubated at different temperatures for 30 min and the remaining phospholipase activity was measured under standard conditions. All measurements are performed using Egg-PC.

Fig.5. Effects of calcium and bile salts on $AsPLA_2$ activity **(A)** Effect of increasing concentration of bile salts (NaDOC) on $AsPLA_2$. PLA_2 activity was measured using Egg-PC emulsion as substrate at pH 8.5 and at 50°C in the presence of 8 mM Ca^{2+}. **(B)** Effect of Ca^{2+} concentration on $AsPLA_2$ activity. $AsPLA_2$ activity was measured at various concentrations of

Ca^{2+} using Egg-PC emulsion as substrate at pH 8.5 and at 50°C (also at 37°C) in the presence of 8 mM NaDOC.

Fig.6. Variations in $AsPLA_2$ activity on DLPC, DLPE, DLPG and DLPS monolayer's with the surface pressure. Enzymes were injected into the reaction compartment of a zero order trough (volume, 130 ml; surface area, 108.5 cm^2; buffer: 10 mM Tris-HCl, (pH 8), 150 mM NaCl, 21 mM $CaCl_2$, and 1 mM EDTA). Activities were expressed as the number of moles of substrate hydrolyzed per time unit (min) and surface unit (cm^2) at the appropriate enzyme concentrations. The activity values were presented as the means of duplicate experiments.

Fig.7. Homology models of the PLA_2 proteins from annular and white seabreams. **(A)** The non-identical amino acids to the human PLA_2 of the solvent accessible surface are mapped on the structure. **(B)** The homology model generated by MODELLER was superposed with the human PLA_2 crystal structure (Transparent structure) using in VMD 1.8.2 molecular viewer. The catalytic dyad is shown in stick representation and the Ca^{++} ions are shown in green. **(C)** The molecular surfaces of the three $sPLA_2$ structures are colored according to the Kyte-Doolittle hydrophobicity scale using Chimera 1.8 molecular viewer. Orange patches on the surface represent the most hydrophobic residues.

Fig.8. Interaction model of POPC and POPG ligands with $AsPLA_2$ and molecular dynamics of the $AsPLA_2$/POPC complex performed over 30 ns simulation at different temperature. **(A)** Interaction model of POPC and POPG ligands with $AsPLA_2$. Molecular docking complexes with the $AsPLA_2$ refined with molecular dynamics. The H_1, H_2, H_3 and the rest of the protein segments are colored in red, green, yellow and light blue respectively. The residues with lesser or equal than 4 Å of distance to any of the ligand atoms are represented in sticks. **(B)** Molecular dynamics of the $AsPLA_2$/POPC complex performed over 10 ns simulation at 38 and 51 °C (311 K and 324 K). Cα RMSD time evolution and Root Mean Square Fluctuation profiles (RMSF) at 38 and 51 °C (311 K and 324 K) were conducted. The 67-70 loop is marked with gray boxes.

(C) The Cα atomic fluctuation values were mapped on the protein structure in which the most flexible segments are colored in red.

Figure 1

A)

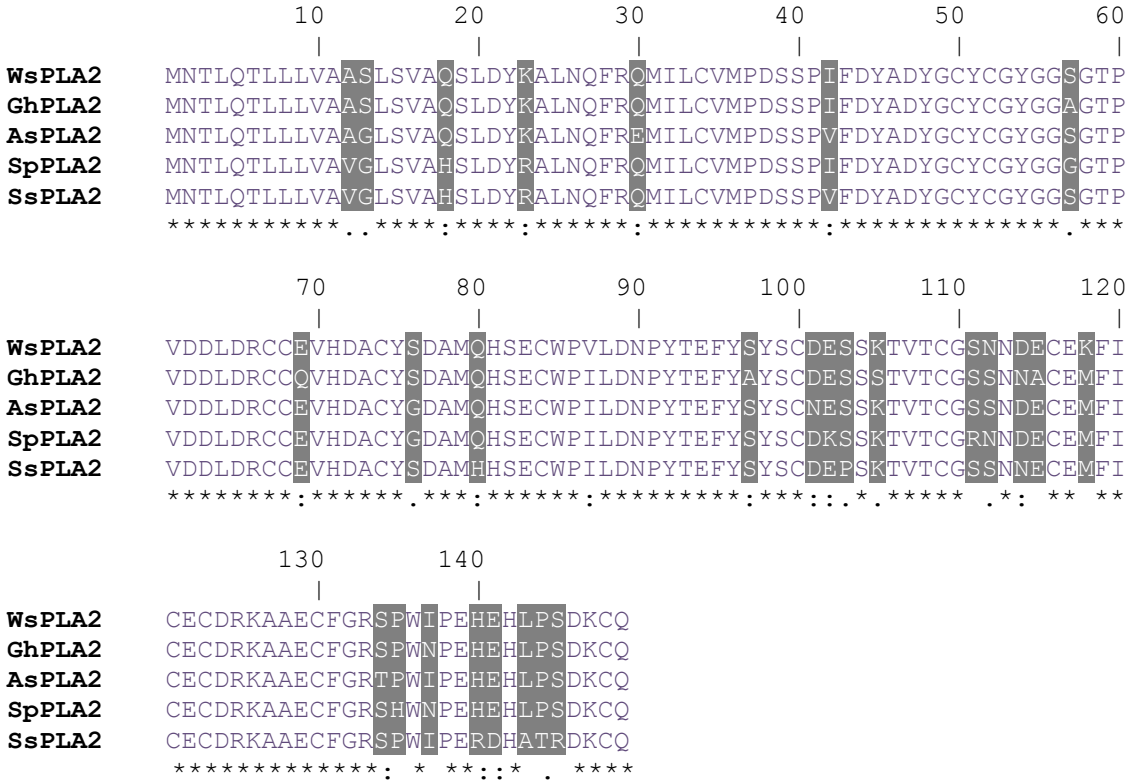

B)

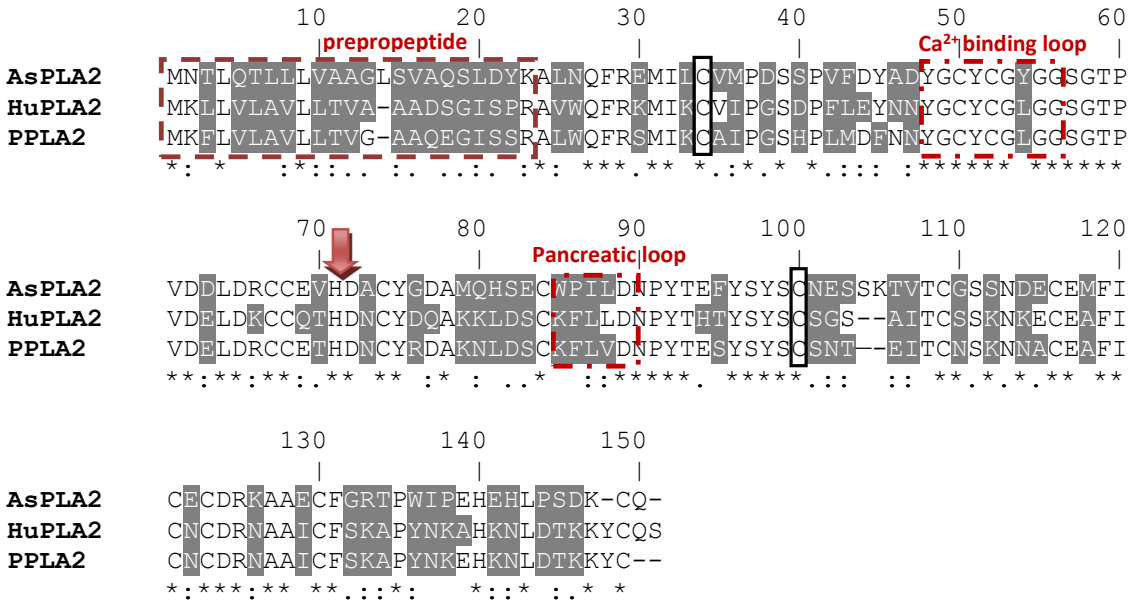

Figure 2

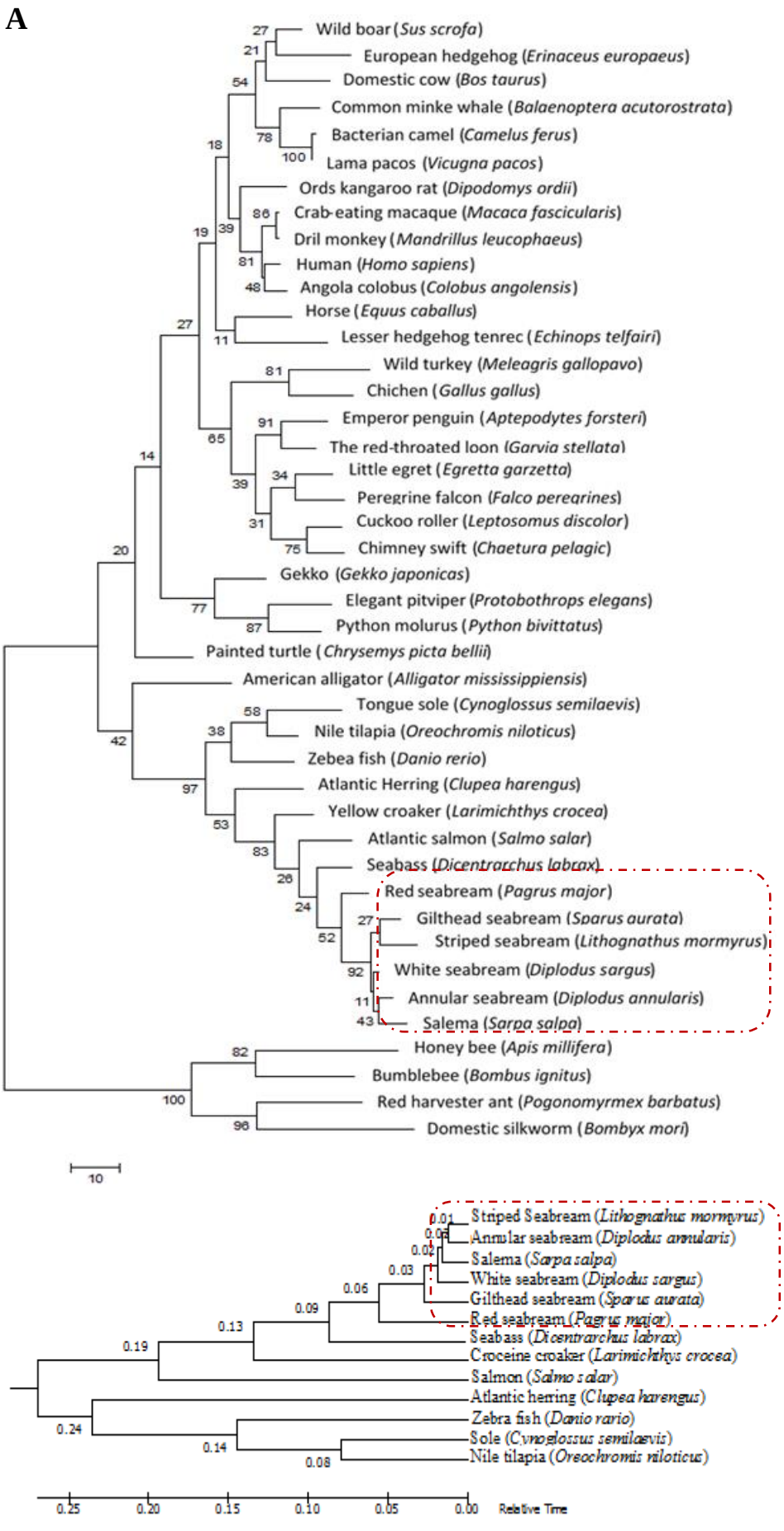

Figure 3

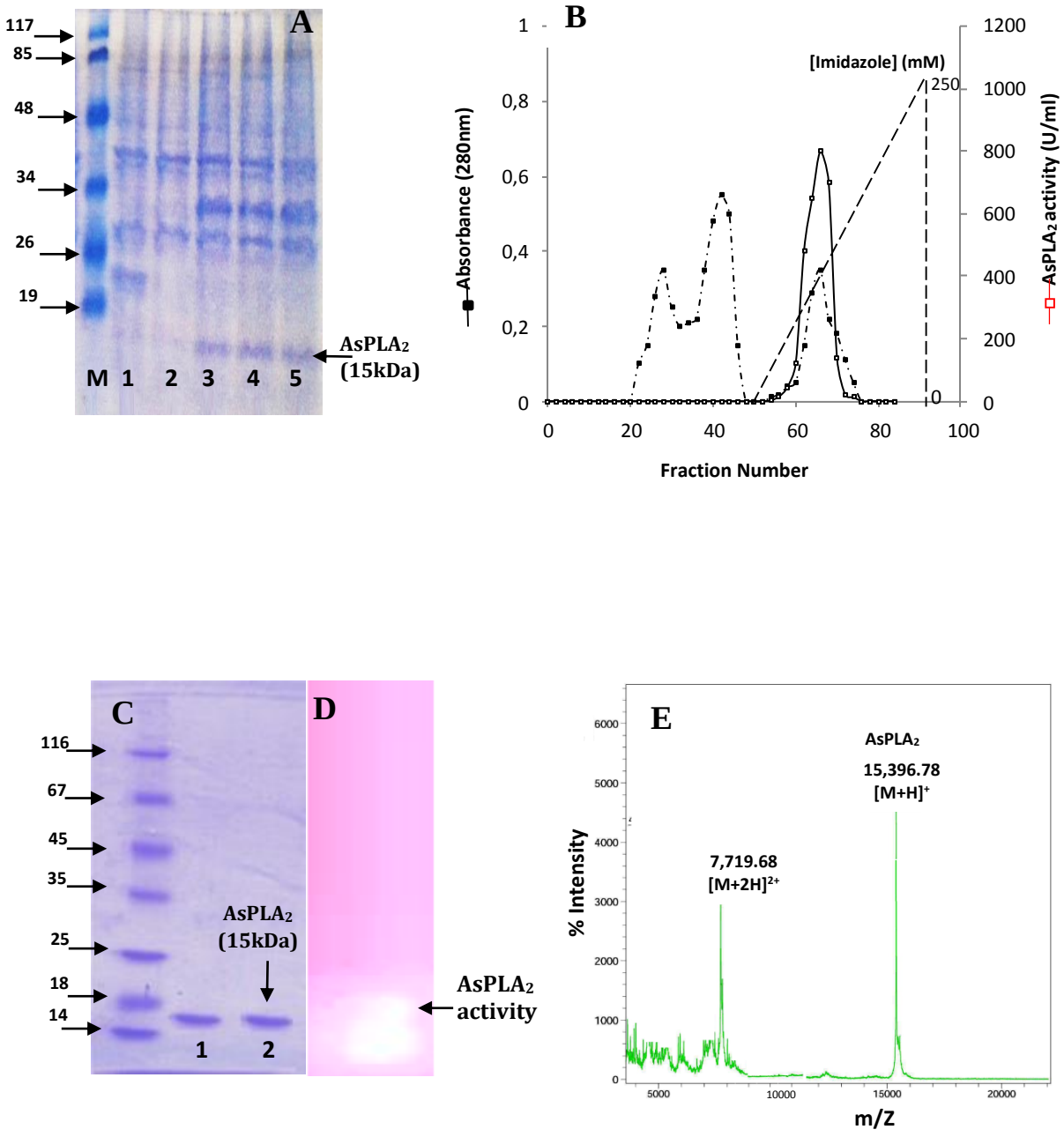

Figure 4

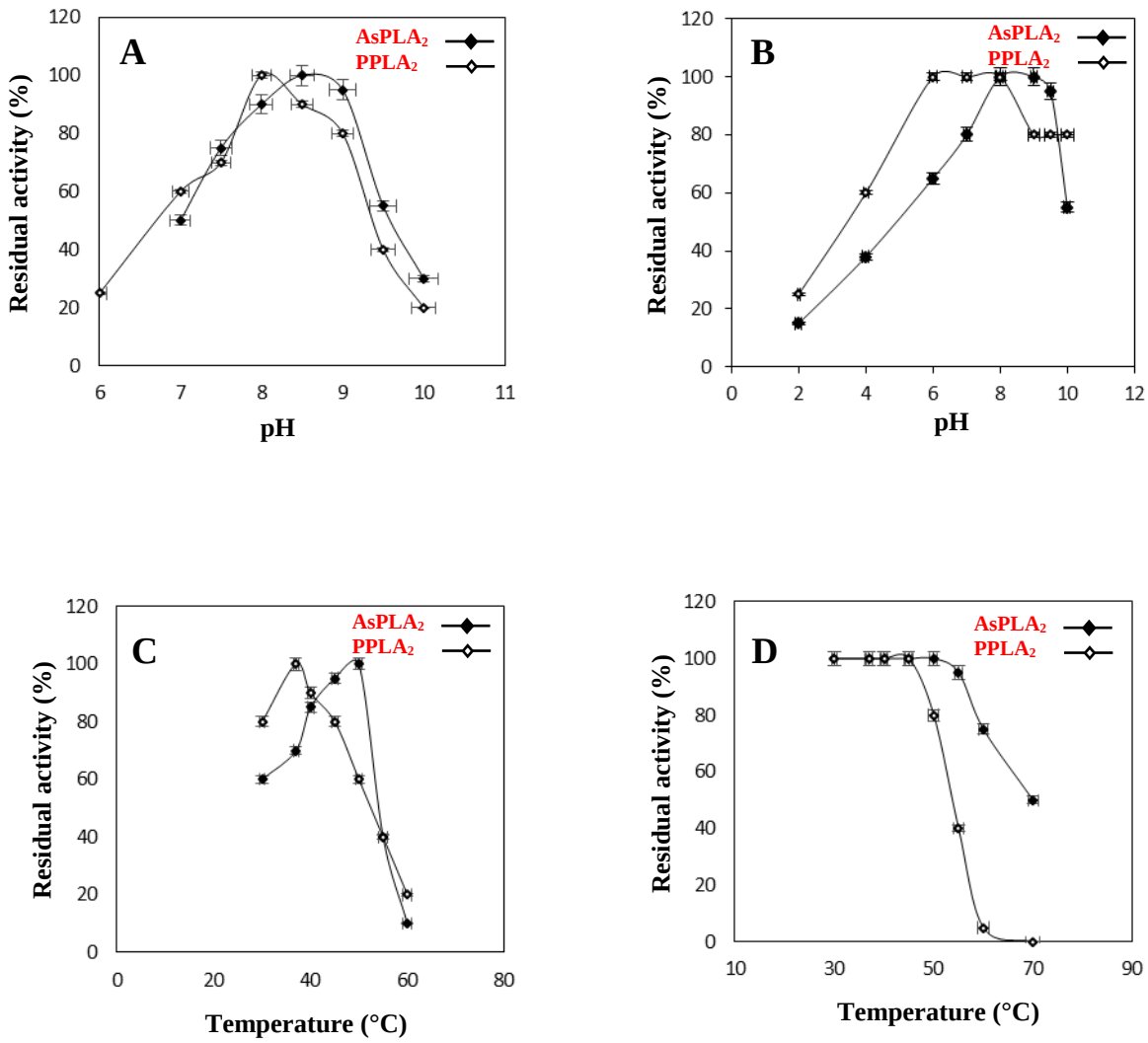

Figure 5

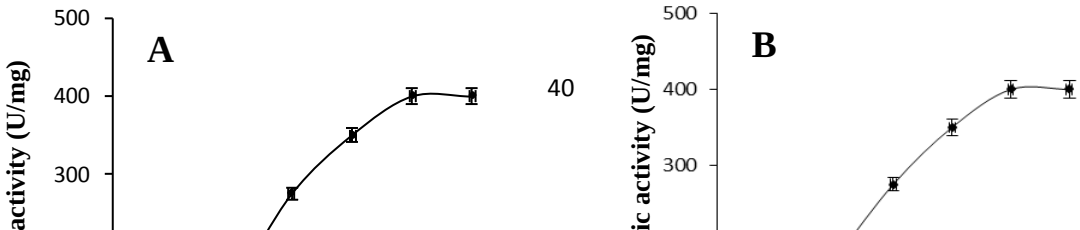

Calcium concentration (mM)

Figure 6

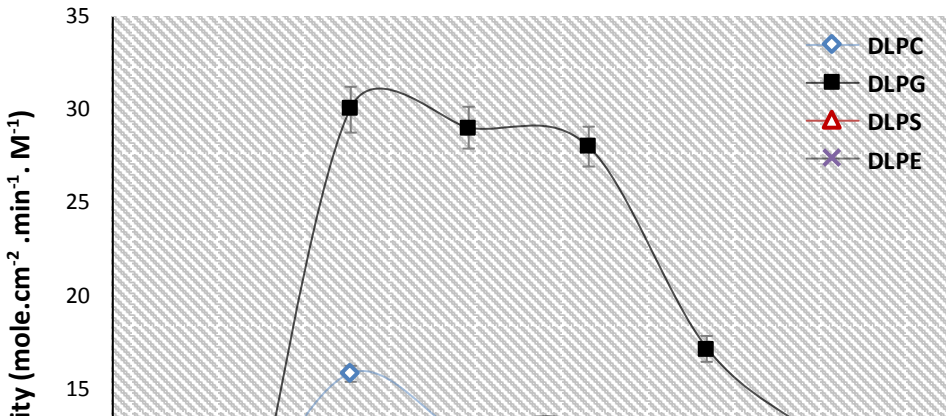

Figure 7

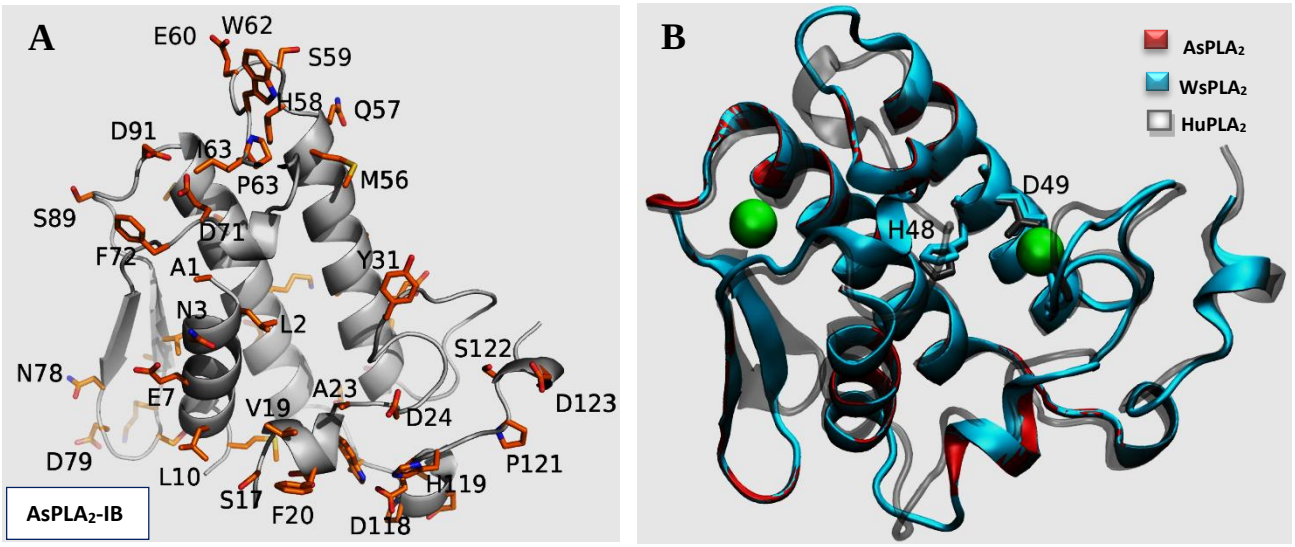

Figure 8

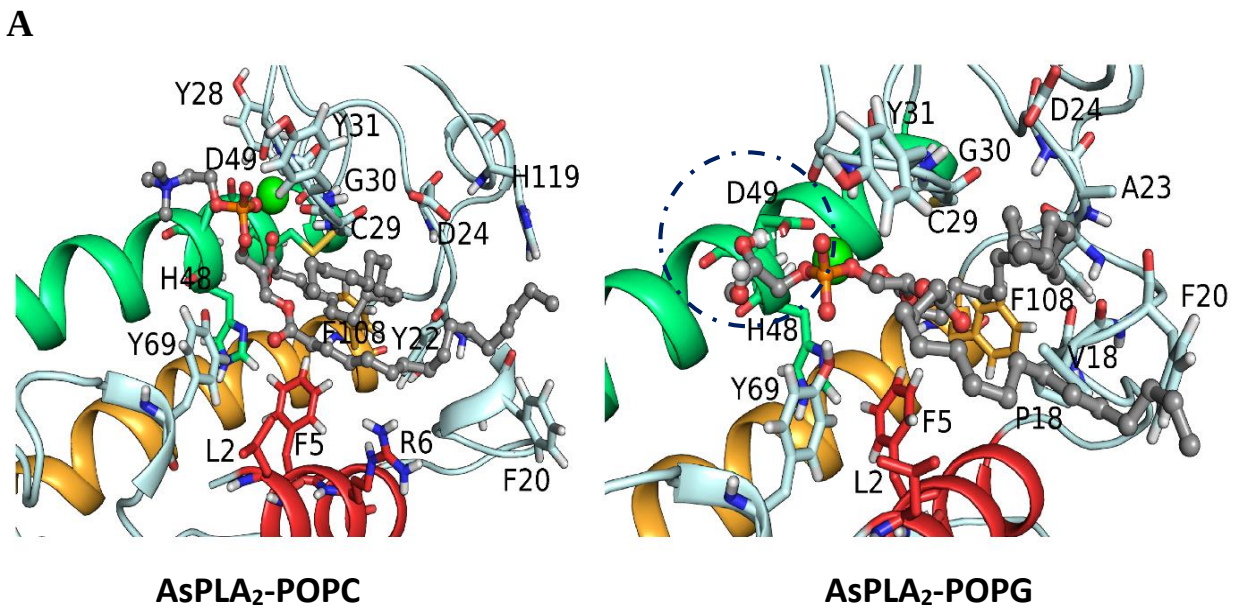

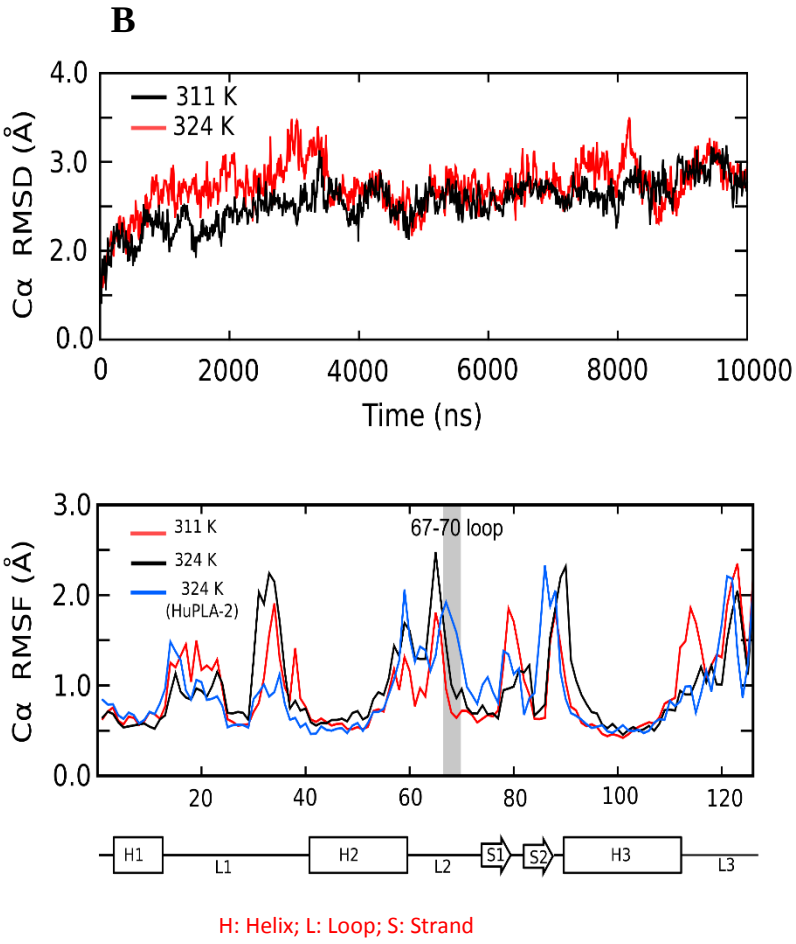

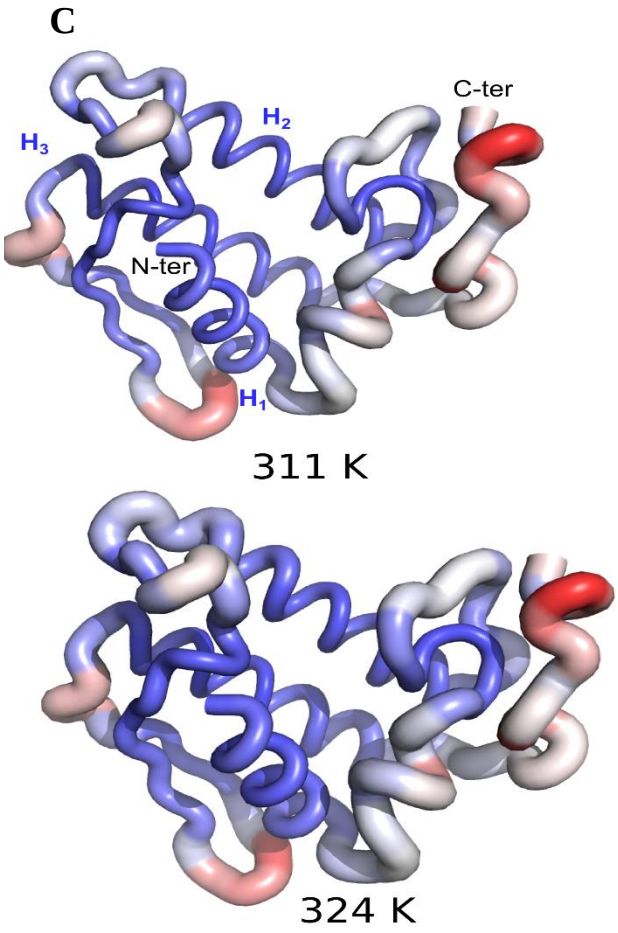

Table 1 Primers used in the cloning and expression of genes encoding mature Sparidae phospholipases.

Cloning Primers	
Forward	5'- **ATG** AAT ACC CTC CAG ACT CTC -3'
Reverse	5'- GACTCGAGTCGACATCGA -3'
Expression primers	
Forward	5'- GAT**CCCATG**GGCACTCAACCAGTTC AGA G-3'
Reverse	5'- GATC**GCGGCCGC**GTTGACACAATGGACTTT-3'

Restriction sites *NcoI* and *NotI* are underlined.

Table 2 Flow sheet of $AsPLA_2$ purification

Purification steps	Protein[a] (mg)	Specific activity [(b)] (U/mg)	Overall Yield (%)
Inclusion bodies solubilization	26	-	-
Refolded enzyme after dialysis	18	240	100
Affinity column	13	440 400 (*)	72

(a) Proteins were estimated by Bradford method [20]. The experiments were conducted three times.

(b) 1 Unit: µmole of fatty acid released per mg of protein using Egg-PC emulsion as substrate in the presence of 6 mM NaDOC and in the presence of 10 mM $CaCl_2$. (*) This value was obtained using egg yolk emulsion under the same condition.